Inorganic Chemistry

ARTICLE

pubs.acs.org/IC

Sulfur Dioxide in Water: Structure and Dynamics Studied by an Ab Initio Quantum Mechanical Charge Field Molecular Dynamics Simulation

Syed Tarique Moin,[†] Len Herald V. Lim, Thomas S. Hofer, Bernhard R. Randolf, and Bernd M. Rode*

Theoretical Chemistry Division, Institute of General, Inorganic and Theoretical Chemistry, University of Innsbruck, Innrain 52a, A-6020 Innsbruck, Austria

ABSTRACT: An ab initio Quantum Mechanical Charge Field Molecular Dynamics Simulation (QMCF MD) was performed to investigate structure and dynamics behavior of hydrated sulfur dioxide (SO_2) at the Hartree−Fock level of theory employing Dunning DZP basis sets for solute and solvent molecules. The intramolecular structural characteristics of SO_2, such as S═O bond lengths and O═S═O bond angle, are in good agreement with the data available from a number of different experiments. The structural features of the hydrated SO_2 were primarily evaluated in the form of $S-O_{wat}$ and $O_{SO_2}-H_{wat}$ radial distribution functions (RDFs) which gave mean distances of 2.9 and 2.2 Å, respectively. The dynamical behavior characterizes the solute molecule to have structure making properties in aqueous solution or water aerosols, where the hydrated SO_2 can easily get oxidized to form a number of sulfur(VI) species, which are believed to play an important role in the atmospheric processes.

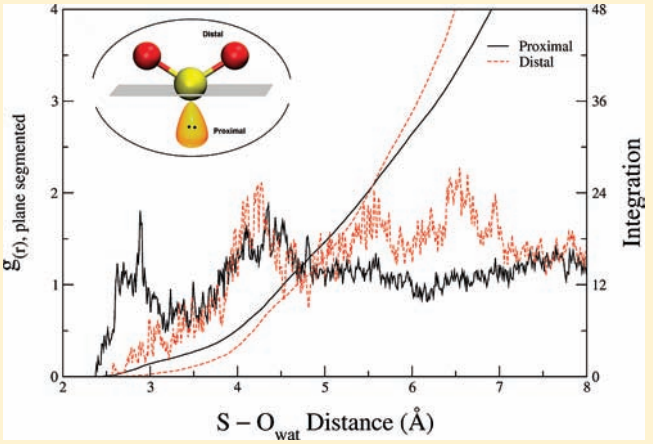

1. INTRODUCTION

Sulfur dioxide plays a major role in the global sulfur cycle, forms acid rain, and is also an important industrial product.[1−3] Because of the highly polar nature of SO_2 and H_2O, the interaction of SO_2 with water leads to formation of weak acidic solutions.[4] The solutions contain mainly solvated SO_2 and minor concentrations of sulfurous acid ($H_2SO_{3(aq)}$) and other anions, such as sulfite SO_3^{2-}, sulfonate ion (HSO_3^-) and its tautomeric form bisulfite (SO_3H^-). Different types of sulfur species, notably SO_2 and H_2S, exist in the atmosphere, in particular in the troposphere, and they are produced by biogenic activity, volcanic eruptions, and combustion of fossils fuel. Oxidation of SO_2 and H_2S in the presence of water results in the acid rain which is also termed as "wet" deposition of sulfur species.[5−8] The mechanism for the oxidation of SO_2 to SO_3 was proposed by Stockwell and Calvert.[9,10] Further reaction of gaseous SO_3 in water vapors results in the formation of sulfate and sulfuric acid aerosols in the Earth's atmosphere.[9,11−13] Hydrate forms of this acid are capable of promoting the growth of new particles via both binary homogeneous and heterogeneous nucleation which involve the reaction of SO_3 with aqueous acid droplets and the condensation of sulfuric acid vapors on pre-existing aerosols particles. These particles can influence climate by scattering solar radiation and therefore, act as cloud condensation nuclei.[14] Consequently, the amount of sunlight reaching Earth's surface is decreased, which ultimately tends to reduce the surface temperature, and this phenomenon is also named as "global dimming".[15,16] In such a way, SO_2 indirectly plays a very significant role in aqueous environment, therefore, it seems important to investigate the SO_2/H_2O system in detail. Symmetry considerations indicate that SO_2 belong to the C_{2v} point group whereas CO_2 has $D_{\infty}h$ symmetry. The difference in structure between SO_2 and CO_2 can also be explained by their molecular shapes. The SO_2 is a bent molecule because of the electron lone pair on the sulfur atom. The central carbon atom of CO_2 has two electron domains which make the molecule nearly linear compared to SO_2 having three electron domains around the sulfur atom. This contrasting character between these two molecules will certainly affect their hydration behavior which is analyzed in terms of structure and dynamics.

A number of studies on structure and energetics of SO_2-H_2O complexes have been reported using experimental and theoretical approaches.[17−23] Liquid SO_2 has also been studied via molecular dynamics simulations to evaluate thermodynamic, structural, and dynamical properties.[24,25] Several spectroscopic investigations as well as X-ray and Neutron Diffraction were also employed to investigate physicochemical properties of the liquid SO_2.[26−32] There is also spectroscopic and computational evidence for SO_2 ionization at 128 K of ice nanoparticles which indicate that the solvation of an anion such as HSO_3^- by molecular SO_2 adsorbate facilitates the SO_2 ionization process

Received: November 8, 2010
Published: March 18, 2011

at the ice surface.[33] Theoretical studies on the addition of H_2O and OH to SO_2 were also carried out to explore the mechanism for the formation of other sulfur products, such as sulfonate, H_2SO_3, and $HOSO_2$ radical.[34,35] The central role of sulfur species in many atmospheric processes is believed to be understood as SO_2 interactions at aqueous interfaces, but its role in aqueous solutions will be helpful to explore the overall hydration behavior of the solute, which upon hydration readily tranforms into different sulfur species. As mentioned earlier, SO_2 indirectly plays very significant roles in the atmospheric environment, and this study was carried out to emphasize the characteristic behavior of SO_2 in connection with water. For this purpose, an ab initio Quantum Mechanical Charge Field Molecular Dynamics Simulation (QMCF MD) was performed with a single SO_2 molecule in water to investigate the structure and dynamics of hydrated SO_2 as the detailed structural and dynamical features of hydrated SO_2 can be helpful to elucidate the role of SO_2 embedded in water either in solution or in aerosols and hence to obtain a better understanding of the aforementioned atmospheric phenomena.[36−38]

2. METHODS

Simulation Method. The ab initio Quantum Mechanical Charge Field Molecular Dynamics (QMCF MD) is an advanced approach of the QM/MM MD simulation method without the need for constructing force field potentials of solute−solvent interactions, thus requiring only solvent−solvent interaction potentials.[36−38] The QMCF MD code has an interface to the parallel version of the QM program "TURBOMOLE" for the quantum chemical calculations.[39] The inner core and extended layer zone constitute the chemically most relevant region which is treated quantum mechanically. It contains the solute molecule along with the full hydration shell while the remaining system is treated by the solvent potential, in our case by the flexible BJH−CF2 water model.[40,41] The ab initio Hartree−Fock (HF) level of theory for the QM regions employing Dunning double ξ plus polarization basis sets has proved to be the best compromise between accuracy and computation cost.[42−45] The point charges assigned to atoms in the Molecular Mechanical region that dynamically change their positions are incorporated via a perturbation term in the core Hamiltonian for the QM region, which is an important feature of the QMCF MD methodology.

$$V' = \sum_{J=1}^{M} \frac{q_J}{r_{iJ}} \quad (1)$$

The Coulomb interactions between atoms in the QM and MM regions are described by the dynamical fluctuating charges of the QM atoms derived from Mulliken population analysis which has proved the best compatibility with the flexible BJH−CF2 water model, thus considering all polarization and charge transfer effects.[46] The forces considered in the core zone are quantum mechanical and Coulomb forces whereas in the layer zone, besides these forces, non-Coulomb forces between layer zone and the solvent molecules in the Molecular Mechanical region are also taken into account. The forces on particles in the Molecular Mechanical region are calculated by the selected water model (BJH) augmented by Coulomb and non-Coulomb contributions from the QM region. To ensure a smooth transition of solvent molecules between QM and MM region, a smoothing function $S(r)$ is also applied in this approach. The details of the method are given in ref 37.

The appropriate selection of basis sets is a critical factor to carry out a successful QMCF MD simulation. Therefore, geometry optimization calculations were performed for a gas phase SO_2, as well as with continuum solvent modeled by a self-consistent reaction field (SCRF) at different levels of theory employing Dunning DZP basis sets, to produce the structural features compared to experimental values.[47]

Table 1. Intramolecular Structural Features of SO_2 Evaluated from QMCF MD Simulation in Comparison to the Values Obtained from Optimization Calculations and Experiments[a]

method(basis sets)	S═O bond length [Å]	O═S═O angle [deg]
Gas Phase		
MP2(DZP)	1.47	119.0
CCSD(DZP)	1.45	118.7
HF(DZP)	1.41	118.5
SCRF		
MP2(DZP)	1.47	117.5
CCSD(DZP)	1.45	116.8
HF(DZP)	1.41	116.5
Experiments		
X-ray crystallography[64]	1.43 ± 0.015	119.5 ± 1.5°
electron diffraction[65]	1.43 ± 0.01	120 ± 5°
microwave spectrum[66]	1.4321	119°2.1′
X-ray (liquid)[32]	1.42(1)	
electron diffraction (gaseous)[67]	1.4343(2)	119.5(3)
neutron diffraction (liquid)[32]	1.42(2)	121(3)
XANES spectrum (gaseous)[61]	1.432	119.53
QMCF MD	1.415 ± 0.075	116.2 ± 8°

[a] The values in parentheses are their estimated standard deviations.

The calculated S═O bond lengths are given with the experimentally determined values summarized in Table 1. The S═O bond lengths calculated at the HF level of theory in gas phase and with the SCRF model are slightly shorter than the experimental values while the correlated ab initio methods slightly overestimate them. Table 2 shows interaction energies calculated for 1:1 SO_2−H_2O complex at the HF, MP2, and CCSD level of theory employing DZP basis sets for all atoms of the cluster. The interaction energy obtained at the HF level of theory is very close to the CCSD value whereas MP2 shows underestimation in the calculated energy. The HF level of theory with the Dunning DZP basis set was thus considered appropriate for the QMCF MD simulation of SO_2 immersed in water molecules. Although H-bonds result slightly too weak and flexible at the HF level compared with those of the correlated methods, but this error is less serious than the too rigid structures of H-bonded systems resulting from DFT methods.[48−50]

Analysis. The structural properties of the sulfur dioxide in solution were evaluated by radial distribution functions (RDFs) and angular distribution functions (ADF). Mean residence time (MRT) of ligands in the hydration shell were determined from the trajectories sampled over 10 ps for t^* values of 0.0 and 0.5 ps, denoted as $\tau^{0.0}$ and $\tau^{0.5}$ in ps utilizing the direct method.[51] The ratio of the number of all transitions occurring through a shell boundary to the number of changes persisting longer than 0.5 ps, is termed R_{ex}. It counts the number of attempts for migration of water ligands required to achieve one lasting exchange event.

$$R_{ex} = \frac{N_{ex}^{0.0}}{N_{ex}^{0.5}} \quad (2)$$

where $N_{ex}^{0.0}$ and $N_{ex}^{0.5}$ are the number of exchange events occurred for t^* 0.0 and 0.5 ps, respectively.

Simulation Protocol. The simulation was carried out in the canonical NVT ensemble with periodic boundary condition for a box containing one SO_2 molecule and 999 water molecules. This simulation box is a cube of 31.05 Å side lengths having density of 0.997 g/cm^3, corresponding to that of water at ambient condition. The Newtonian

dx.doi.org/10.1021/ic102240p |Inorg. Chem. 2011, 50, 3379–3386

equations of motion were integrated with a time step of 0.2 fs using a second-order Adams−Bashforth predictor−corrector algorithm. The Berendsen algorithm with coupling constant of 0.2 ps was employed to keep the temperature at 298 K.[52] The reaction field method was used to address the long-range Coulomb interactions for which the cutoff distance was set to 15.0 Å whereas for non-Coulomb interactions cutoff distances of 5.0 and 3.0 Å were used for O−H and H−H interactions among water molecules, respectively. The BJH−CF2 water model includes intramolecular parameters, thus providing the full flexibility specially needed for smooth transitions between QM and MM regions.[40,41] The radius of the core zone was 3.0 Å, the layer zone extended to 5.7 Å, and the smoothing region had a thickness of 0.2 Å ranging from 5.5 to 5.7 Å. The gas phase optimized structure of a SO_2 molecule immersed in a pre-equilibrated water box was subjected to thermal equilibration at 298.16 K for 10 ps, followed by a sampling of 10 ps.

Table 2. Interaction Energies and Structural Features Calculated for 1:1 SO_2−H_2O Complex at Different Level of Theory Employing DZP Basis Set for All Atoms of the Cluster

		structural features	
level of theory	interaction energies (kcal/mol)	S═O bond length [Å]	O═S═O angle [deg]
HF	−5.67	1.41	117.8
MP2	−5.24	1.47	118.5
CCSD	−5.66	1.45	117.9

3. RESULTS AND DISCUSSION

Structure. The structural features of SO_2 obtained from the QMCF MD simulation are in good agreement with the experimental data (cf. Table 1). The RDFs between atomic pairs of SO_2

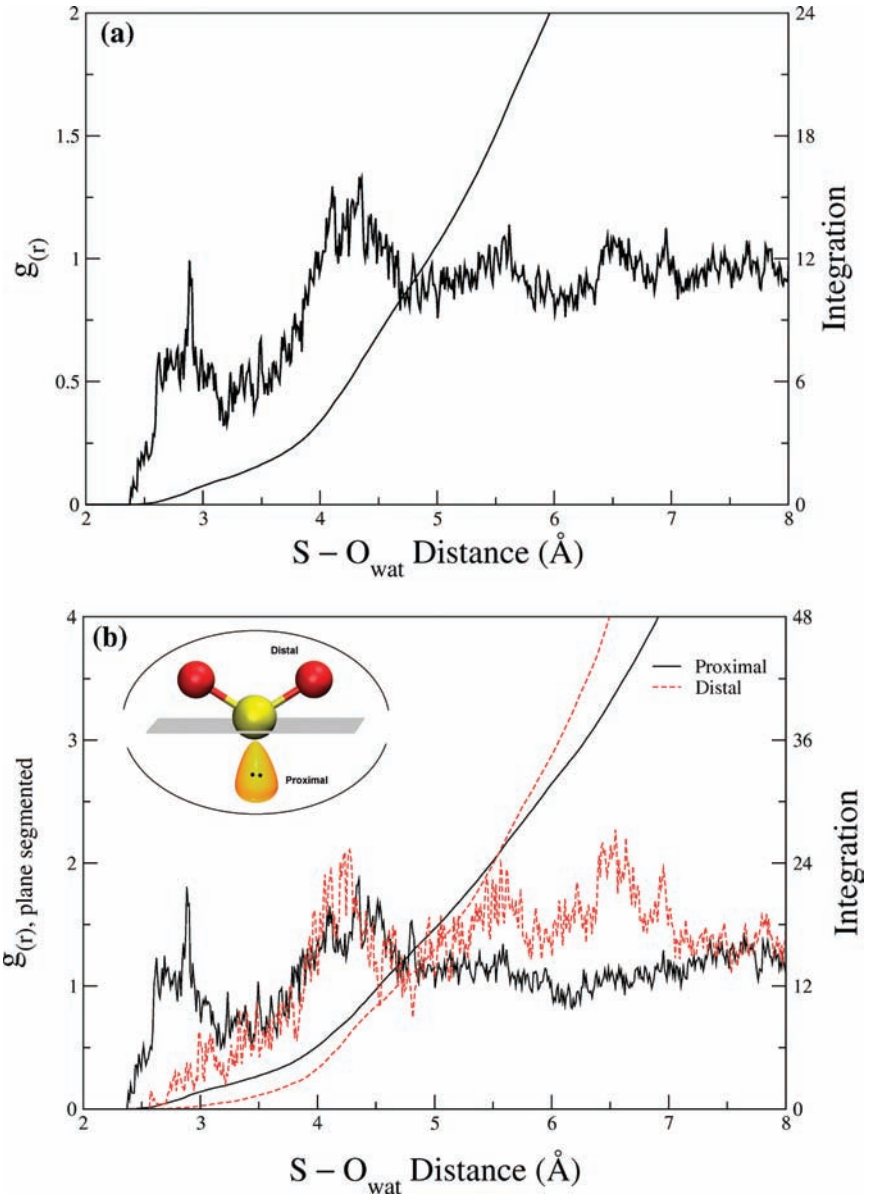

Figure 1. RDF between (a) sulfur atom of SO_2 and oxygen atoms of water molecules and (b) plane segmented S−O_{wat} RDFs for two hemispheres, the proximal and the distal.

dx.doi.org/10.1021/ic102240p |Inorg. Chem. 2011, 50, 3379–3386

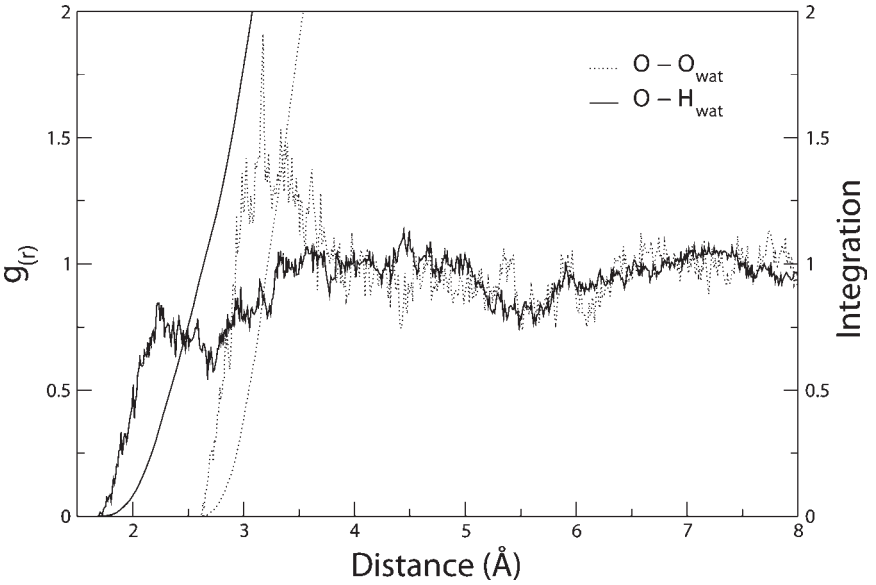

Figure 2. RDF between oxygen atoms of SO_2 and hydrogen and oxygen atoms of water molecules.

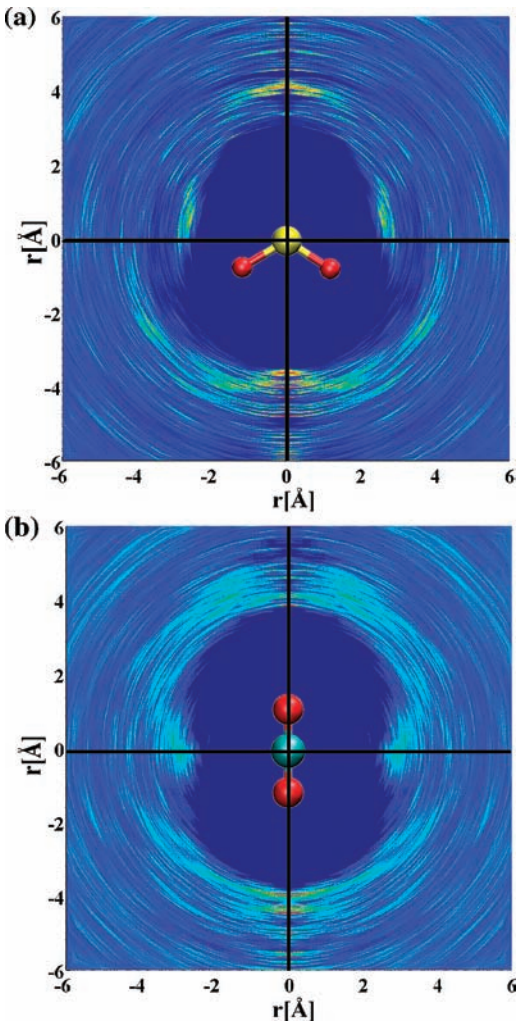

Figure 3. Contour maps obtained from ARD analysis showing the difference in the hydration shell of the (a) SO_2 and (b) CO_2. Color keys; blue = low intensity; red = high intensity.

and water molecules were plotted to explore the structural features of hydrated SO_2. The total S−O_{wat} RDF exhibits a broad peak between 2.3 and 4.7 Å with a strong shoulder peak at 2.9 Å as shown in Figure 1a. Integration of this RDF up to the minima after the shoulder peak and the major broad peak yielded ∼4 and ∼10 water molecules, respectively. The S···O_{wat} mean distance deduced from the shoulder peak of the S−O_{wat} RDF correlates with experimental data available for SO_2−H_2O complexes.[20] Beside the experimental observation, the S−O_{wat} RDF plot from the QMCF MD simulation is in reasonable agreement with the RDF in the bulk condition, evaluated for sulfur dioxide at the air/water interface using molecular dynamics with KS-DFT and classical polarizable interaction potentials.[53] A detailed analysis was also performed to interpret the shoulder peak which is indicative of two different types of hydration because of nonlinearity of the SO_2 molecule. This was accomplished by plane-wise partitioning of the simulation box into two subregions by defining a plane centered at the sulfur atom with a normal vector resulting from the sum of the two S═O vectors. Thus, the system was separated into a proximal and a distal hemisphere (see Figure 1b), enabling the decomposition of the overall RDF. The mean distances between sulfur and water oxygens were centered at 2.9 and 4.3 Å, corresponding to the shoulder peak and a broad peak belonging to the "proximal" and "distal" hemishpere, respectively (cf. Figure 1b). The splitting of RDF analysis into two different domains unfolded the asymmetric hydration behavior of the solute.

The characteristic features of the hydration layer were also elucidated using the sectorial RDF defined by a S═O bond vector of the O═S═O. The chemically equivalent nature of each oxygen atom of the solute led to calculate the average O−O_{wat} and O−H_{wat} RDF, which served to determine the existence of hydrogen bonds between solute and solvent molecules (Figure 2). A wide peak from 2.6 to 3.9 Å was observed in the O−O_{wat} RDF whereas the mean distance between the hydrogen of water molecules and oxygen of SO_2 was evaluated as 2.2 Å, deduced from the distinct peak observed in the O−H_{wat} RDF. The O−O_{wat} and O−H_{wat} RDF plots were integrated to ∼1 water molecule bound to each oxygen atom of SO_2 molecule making hydrogen bonds. The

dx.doi.org/10.1021/ic102240p |*Inorg. Chem.* 2011, 50, 3379–3386

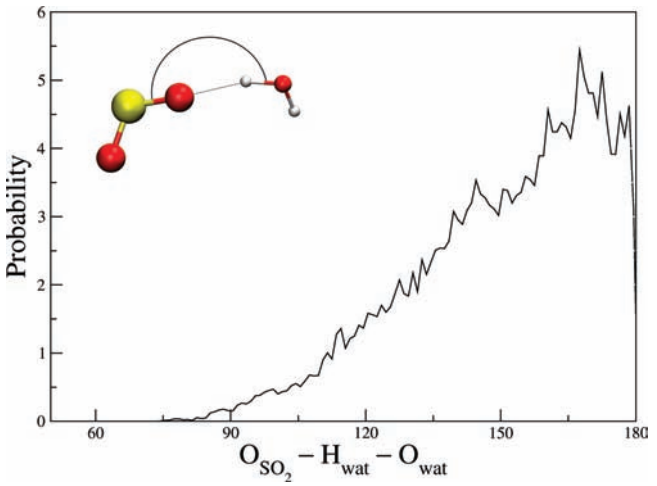

Figure 4. Normalized ADF (ADF_{norm}) of $O_{SO_2}-H_{wat}-O_{wat}$ angle between SO_2 and water molecules.

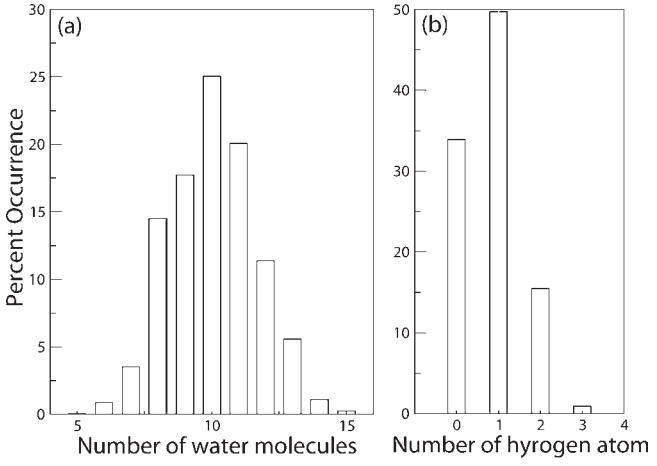

Figure 5. Coordination number distributions of (a) water molecule surrounding the whole SO_2 molecule and (b) hydrogen atoms bound to each oxygen of SO_2.

$O-H_{wat}$ bond distance of 2.2 Å indicates that explicit hydration of SO_2 influences the geometrical arrangement of hydrates and leads to different numbers of hydrogen bonds. With increasing number of water molecules, the strength of hydrogen bonds increases reflected by the short $O-H_{wat}$ bond distance. This observation is in fair agreement with the theoretical study performed on sulfur dioxide-water clusters ($SO_2 \cdot nH_2O$) to evaluate structure and energetics of hydrated species.[21]

To further verify the difference in the distribution of solvent molecules, conical regions surrounding the SO_2 atom have been defined. The sum of the two S═O vectors acted as an axis for the cones, the angle increment of the cones was set to 10°. Evaluation of RDFs within the defined cone-segments enable the analysis of the angular-radial distributions (ARDs) of the system (see Figure 3). The varying arrangement of solvents around sulfur dioxide was also compared with the symmetric ligand density distribution around CO_2 which has nearly linear structural attributes (cf. Figure 3b). The hydration properties of SO_2 analyzed by ARD exhibited asymmetric distribution of solvent molecules illustrated by the contour plot in Figure 3a. The

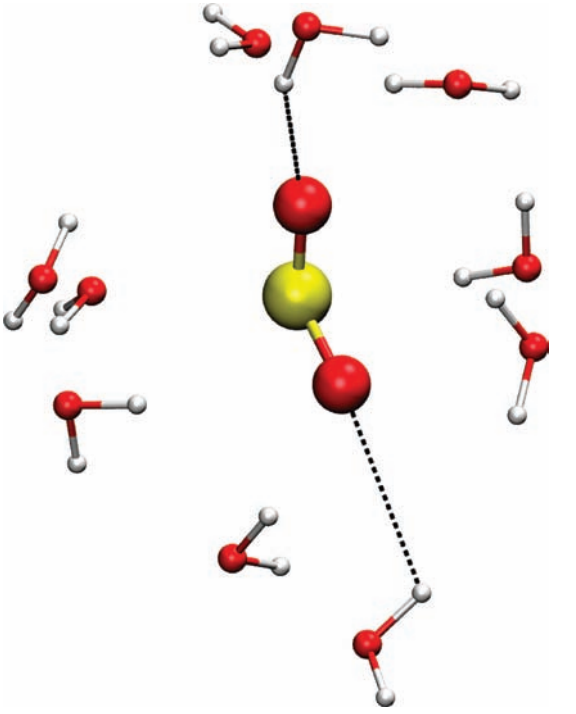

Figure 6. Snapshot of the SO_2 molecule surrounded by hydration layer.

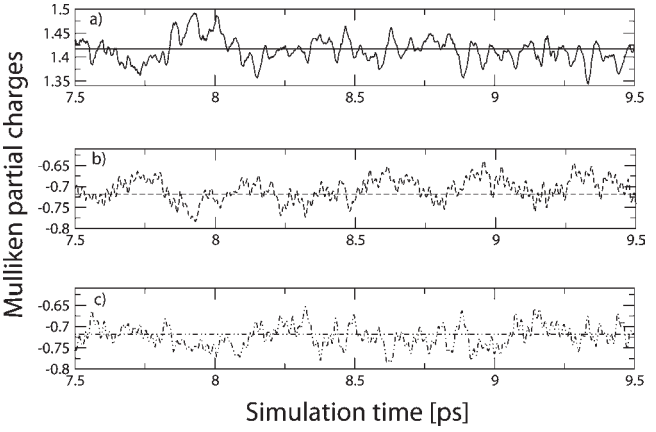

Figure 7. Fluctuation of partial atomic charges of all three atoms of the SO_2 molecule: (a) sulfur atom, (b) and (c) oxygen atoms.

solvent density in the hydration shell was reduced at the proximal side because of the influence of the electron lone pair on the sulfur atom of SO_2. This was attributed by the hollow cavity or empty space at the proximal side (shown above the horizontal line bisecting the plot into two distinct sides) compared to the distal one where oxygens of sulfur dioxide interact with water molecules via H-bonds indicated by high solvent density distribution. Figure 4 shows the normalized ADF (ADF_{norm}) for the $O_{SO_2}-H_{wat}-O_{wat}$ angle depicting the existence of hydrogen bonds between solute and solvent molecules. The highest angular probability of this angle at ~167.5° characterizes the linearity of these hydrogen bonds. The strength of hydrogen bonds between sulfur dioxide and water molecules is also evident from the ADF_{norm}.

The hydration shell surrounding the whole SO_2 molecule was also analyzed in terms of the coordination number distribution

dx.doi.org/10.1021/ic102240p |*Inorg. Chem.* 2011, 50, 3379–3386

(CND), leading to a variation between 5 and 15, with an average value of 10 as presented in Figure 5a. The average number of hydrogen atoms of water molecules interacting with each oxygen atom of SO_2 was evaluated as 0.8 with a CND ranging from 0 to 3 (cf. Figure 5b) using the cutoff limit of 2.5 Å, adopted from the $g(r)$ functions (see Figure 2). The highest probability of one hydrogen atom bound to each oxygen of the solute indicates more or less constant existence of two hydrogen bonds between solute and solvent molecules. The snapshot shown in Figure 6 visualizes the overall hydration shell surrounding the whole solute as well as the hydrogen bonding between oxygens of solute and hydrogen atoms of solvent molecules. The interactions of the SO_2 molecule with water lead to numerous possibilities of geometrical arrangements, leading to different pathways of SO_2 hydration which can ultimately result in the formation of different sulfur species. This is also reflected by the dynamics of the hydrated SO_2 in the following section.[35]

Dynamics. The fluctuation in the Mulliken partial charges for sulfur and two oxygen atoms of sulfur dioxide was also monitored during the whole simulation and is presented in Figure 7, for a fraction of sampling time. The charge on sulfur atom varies between +1.35 and +1.48 with an average value of +1.41 whereas the oxygen atoms carry an average charge of −0.72 varying from −0.78 to −0.64. These charge variations in every step of the simulation demonstrate the importance of its implementation in the QMCF MD methodology.

Table 3. Characteristic Data for the Hydrogen Bond Dynamics of Hydrated SO_2 in Comparison to Hydrated CO_2 and Pure Water from QMCF MD Simulation

	$N_{ex}^{0.5}$/10 ps	$N_{ex}^{0.0}$/10 ps	$\tau_{0.5}$ (ps)	R_{ex}	ref.
$O_{SO2}\cdots H_{wat}$	4	269	2.44	75	this work
$O_{CO2}\cdots H_{wat}$	3	264	2.04	88	55
pure water	20	131	1.3	6.5	54

Table 3 shows the data related to hydrogen bond dynamics of the hydrated SO_2 in comparison to hydrated CO_2 and pure water. The MRT for the hydrogen atoms in proximity of oxygen atoms of SO_2 was determined as 2.44 ps adopting the cutoff limit of 2.5 Å. The MRT value for the hydrogen bonds is 0.4 and 1.14 ps higher than the values of hydrated CO_2 (2.04 ps) and pure water (1.3 ps), respectively, thus indicating the formation of fairly stable hydrogen bonds.[54] The average lifetime of hydrogen bonds between SO_2 and water molecules was also calculated as 0.83 ps which is also higher than the lifetime of hydrogen bonds in hydrated CO_2 and pure water obtained also by the same simulation technique (0.47 ps) and by experiment.[55,54,56] These dynamics data of the water ligands verify the SO_2 molecule to have potential structure making properties compared to CO_2.

Vibrational Frequencies of Hydrated Sulfur Dioxide. The SO_2 molecule being of C_{2v} symmetry has an inherent dipole moment which is expected to be slightly influenced by interaction with water molecules.[20] Therefore, vibrational frequencies of hydrated SO_2 have been considered, particularly regarding the influence of water molecules on SO_2 in the form of aerosols. The frequencies for symmetric stretch, asymmetric stretch, and bending mode for SO_2 embedded in water were calculated from Fourier transformed velocity autocorrelation functions (VACF) from the 10 ps trajectory of the QMCF MD simulation.[57,58] Normal mode calculations were also performed for gaseous SO_2 at different levels of theory with and without PCM model for comparison with experimental values and other theoretical calculation for all vibrational modes of SO_2 (cf. Table 4).[59] The IR frequencies of SO_2 in solution are in good agreement with the experimental frequencies.[60] Application of the Polarized Continuum Model (PCM) in these calculations slightly shifted these frequencies because of the solvent effects. The frequencies calculated from the QMCF MD simulation present a similar picture of the solvent effects which can be compared to recent data obtained from various experiments for aqueous solution of SO_2 and for SO_2-water clusters as summarized

Table 4. Vibrational Frequencies (cm^{-1}) of SO_2(g) Determined by Experiment and Normal Modes Calculations in Comparison to Values for SO_2 in Water Obtained by Experiment and QMCF MD Simulation[a]

	SO_2 frequency (cm^{-1})					
	gas			PCM		
	S=O ν_{as}	S=O ν_s	O=S=O ν_δ	S=O ν_{as}	S=O ν_s	O=S=O ν_δ
HF	1410	1229	539	1345	1215	527
MP2	1308	1089	494	1307	1122	507
CCSD	1396	1195	529	1359	1197	521
experiment[59]	1361	1151.2	519			
	Hydrated SO_2 frequency (cm^{-1})					
	S=O ν_{as}		S=O ν_s		O=S=O ν_δ	
experiment[60]	1333		1155		528	
$SO_{2(aq)}$[61]	1330		1151		559	
$(H_2O{-}SO_2)$[17]	1337.6		1160.2			
QMCF	1373		1224		549	

[a] Values scaled by factor 0.89 according to refs 68,69.

dx.doi.org/10.1021/ic102240p |*Inorg. Chem.* 2011, 50, 3379–3386

in Table 4.[61,17] There are numerous theoretical studies performed for the evaluation of vibrational frequencies which are in good agreement with our QMCF MD simulation.[22,21,62] All these data comparatively show that the presence of water has only a minor effect on the vibrational modes of SO_2, and hence the infrared absorption of this molecule in aerosols formed in the atmosphere will not change much compared to unhydrated SO_2.

4. CONCLUSION

The application of the QMCF MD methodology enabled an accurate treatment of sulfur dioxide in bulk water, thereby treating SO_2 and its immediate surrounding on a quantum chemical basis. All structural and dynamical characteristics agree well with available experimental data. The structure and dynamical characteristics of the hydrated sulfur dioxide prove a fairly strong association of SO_2 with high abundance of water molecules, forming stronger hydrogen bonds than hydrated CO_2.[55] The simulation results also establish the solute molecule as structure maker in aqueous solution or water aerosols. Although the quantum chemical treatment of sulfur dioxide and its surrounding molecules would enable the formation of hydrolyzed species such as HSO_3^-, no such processs was observed within the simulation time of 10 ps. This finding agrees with studies of $SO_2(H_2O)_n$ clusters via laser pulse spectroscopy demonstrating that surface hydration is dominant and that thus conversion to HSO_3^- ions is a slow process.[63] In the atmospheric processes, aerosol formation is an important phenomenon, and the full hydration of SO_2 and its oxidized products in water has been held responsible for nucleation processes in cloud formation. The presented simulation results are encouraging, therefore, for further studies aimed at elucidating such atmospheric processes in the light of supported experimental and theoretical data.

AUTHOR INFORMATION

Corresponding Author

*E-mail: bernd.m.rode@uibk.ac.at. Phone: +43-512-507-5129. Fax: +43-512-507-2714.

Present Addresses

[†]Dr. Panjwani Center for Molecular Medicine and Drug Research, International Center for Chemical and Biological Sciences, University of Karachi, Karachi 75270, Pakistan.

ACKNOWLEDGMENT

Financial support for this work by the Austrian Science Foundation (FWF) and an Austrian Technology Grant (BMWF/RFTE) for Syed Tarique Moin are gratefully acknowledged.

REFERENCES

(1) Cole, J. A.; Ferguson, S. J. *The Nitrogen and Sulfur Cycles*; Cambridge University Press: Cambridge, 1988.
(2) Möller, D. *Luft: Chemie, Physik, Biologie, Reinhaltung, Recht*; Walter de Gruyter: Berlin, 2003.
(3) Brandt, C.; Eldik, R. V. *Chem. Rev.* **1995**, *95*, 119.
(4) Mondal, M. K. *Fluid Phase Equilib.* **2007**, *253*, 98.
(5) Granat, L.; Rodhe, H.; Hallberg, R. O. In *Nitrogen, Phosphorus, and Sulfur*; Svensson, B. H., Søderlund, R., Eds.; Chapter Global Cycles, Ecological Bulletins: Stockholm, 1976; Vol. 32.
(6) Finlayson-Pitts, B. J.; Pitts, J. N. *Chemistry of the upper and lower atmosphere*; Academic Press: San Diego-London, 2000.
(7) Graedel, T. E.; Crutzen, P. J. *Chemie der Atmosphäre*; Spektrum Akademischer Verlag: Heidelber, Berlin, Oxford, 1994.
(8) Charlson, R. J.; Schwartz, S. E.; Hales, J. M.; Cess, R. D.; Coakley, J. A., Jr.; Hansen, J. E.; Hofmann, D. J. *Science* **1992**, *255*, 423.
(9) Stockwell, E. R.; Calvert, J. G. *Atmos. Environ.* **1967**, *17*, 2231.
(10) Calvert, J. G. *SO2, NO, and NO2 oxidation mechanisms: atmospheric considerations*; Butterworth Publishers: Boston, 1984.
(11) Castleman, A. W., Jr.; Davis, R. E.; Munkelwitz, H. R.; Tang, I. N.; Wood, W. P. *Int. J. Chem. Kinet. Symp.* **1975**, *1*, 629.
(12) Anderson, L. G.; Gates, P. M.; Nold, C. R. In *Biogenic Sulfur in the Enviroment*; Saltzman, E. S., Copper, W. J., Eds.; American Chemical Society: Washington, DC, 1989.
(13) Calvert, J. G.; Lazrus, A.; Kok, G. L.; Heikes, B. G.; Walega, J. G.; Lind, J.; Cantrell, C. A. *Nature* **1985**, *317*, 27.
(14) Pruppacher, H. R.; Klett, J. D.; Wang, P. K. *Aerosol Sci. Technol.* **1998**, *28*, 381.
(15) Stjern, C. W.; Kristjánsson, J. E.; Hansen, A. W. *Int. J. Climatol.* **2009**, *29*, 643.
(16) Lohmann, U.; Feichter, J. *Atmos. Chem. Phys.* **2005**, *5*, 715.
(17) Hirabayashi, S.; Ito, F.; Yamada, K. M. T. *J. Chem. Phys.* **2006**, *125*, 034508.
(18) Nord, L. *J. Mol. Struct.* **1982**, *96*, 27.
(19) Schriver, A.; Schriver, L.; Perchard, J. P. *J. Mol. Spectrosc.* **1988**, *127*, 125.
(20) Matsumura, K.; Lovas, F. J.; Suenram, R. D. *J. Chem. Phys.* **1989**, *91*, 5887.
(21) Steudel, R.; Steudel, Y. *Eur. J. Inorg. Chem.* **2009**, *2009*, 1393.
(22) Cukras, J.; Sadlej, J. *J. Mol. Struct. (Theochem)* **2007**, *819*, 41.
(23) Jursic, B. S. *J. Mol. Struct. (Theochem)* **1999**, *467*, 187.
(24) Sokolic, F.; Guissani, Y.; Guillot, B. *J. Phys. Chem.* **1985**, *89*, 3023.
(25) Ribeiro, M. C. C. *J. Phys. Chem. B* **2006**, *110*, 8789.
(26) Makulski, W.; Jackowski, K. *J. Mol. Struct.* **2004**, *704*, 219.
(27) Jaye, A. A.; Hunt, N. T.; Meech, S. R. *J. Chem. Phys.* **2006**, *124*, 024506.
(28) Kamoun, M. *J. Raman Spectrosc.* **1979**, *8*, 225.
(29) Brooker, M. H.; Eysel, H. H. *J. Phys. Chem.* **1984**, *88*, 6201.
(30) Musso, M.; Aliotta, F.; Vasi, C.; Aschauer, R.; Asenbaum, A.; Wilhelm, E. *J. Mol. Liq.* **2004**, *110*, 33.
(31) Chahid, A.; García-Hernández, M.; Prieto, C.; Bermejo, F. J.; Enciso, E.; Martnez, J. L. *Mol. Phys.* **1993**, *78*, 821.
(32) Yamaguchi, T.; Lindqvist, O.; Dahlborg, U. *Acta Chem. Scand. A* **1984**, *38*, 757.
(33) Jagoda-Cwiklik, B.; Devlin, J. P.; Buch, V. *Phys. Chem. Chem. Phys.* **2008**, *10*, 4678.
(34) Li, W. K.; McKee, M. L. *J. Phys. Chem. A* **1997**, *101*, 9778.
(35) Voegele, A. F.; Tautermann, C. S.; Rauch, C.; Loerting, T.; Liedl, K. L. *J. Phys. Chem. A* **2004**, *108*, 3859.
(36) Hofer, T. S.; Pribil, A. B.; Randolf, B. R.; Rode, B. M. *Adv. Quantum Chem.* **2010**, *59*, 213.
(37) Rode, B. M.; Hofer, T. S.; Randolf, B. R.; Schwenk, C. F.; Xenides, D.; Vchirawongkwin, V. *Theor. Chem. Acc.* **2006**, *115*, 77.
(38) Rode, B. M.; Hofer, T. S. *Pure Appl. Chem.* **2006**, *78*, 525.
(39) Ahlrichs, R.; Bär, M.; Häser, M.; Horn, H.; Kölmel, C. *Chem. Phys. Lett.* **1989**, *162*, 165.
(40) Stillinger, F. H.; Rahman, A. *J. Chem. Phys.* **1978**, *68* (2), 666.
(41) Bopp, P.; Jancso, G.; Heinzinger, K. *Chem. Phys. Lett.* **1983**, *98*, 129.
(42) Dunning, T. H. *J. Chem. Phys.* **1970**, *53*, 2823.
(43) Magnusson, E.; Schaefer, H. F. *J. Chem. Phys.* **1985**, *83*, 5721.
(44) Vchirawongkwin, V.; Pribil, A. B.; Rode, B. M. *J. Comput. Chem.* **2009**, *31*, 249.
(45) Lim, L. H. V.; Bhattacharjee, A.; Asam, S. S.; Hofer, T. S.; Randolf, B. R.; Rode, B. M. *Inorg. Chem.* **2010**, *49*, 2132.
(46) Mulliken, R. S. *J. Chem. Phys.* **1955**, *23*, 1833.
(47) Tapia, O.; Goscinski, O. *Mol. Phys.* **1975**, *29*, 1653.
(48) Xenides, D.; Randolf, B. R.; Rode, B. M. *J. Chem. Phys.* **2005**, *122*, 174506.
(49) Yoo, S.; Zeng, X. C.; Xantheas, S. S. *J. Chem. Phys.* **2009**, *130*, 221102.

(50) Schmidt, J.; VandeVondele, J.; Kuo, I. F. W.; Sebastiani, D.; Siepmann, J. I.; Hutter, J.; Mundy, C. J. *J. Phys. Chem. B* **2009**, *113*, 11959.
(51) Hofer, T. S.; Tran, H. T.; Schwenk, C. F.; Rode, B. M. *J. Comput. Chem.* **2004**, *25*, 211.
(52) Berendsen, H. J. C.; Postma, J. P. M.; Gunsteren, W. F. V.; DiNola, A.; Haak, J. R. *J. Chem. Phys.* **1984**, *81*, 3684.
(53) Baer, M.; Mundy, C. J.; Chang, T. M.; Tao, F. M.; Dang, L. X. *J. Phys. Chem. B* **2010**, *114*, 7245.
(54) Randolf, B. R.; Hofer, T. S.; Rode, B. M., unpublished results.
(55) Moin, S. T.; Pribil, A. B.; Lim, L. H. V.; Hofer, T. S.; Randolf, B. R.; Rode, B. M. *Int. J. Quantum Chem.* **2010**, in press.
(56) Lock, A. J.; Woutersen, S.; Bakker, H. J. *Femtochemistry and Femtobiology*; World Scientific Publication: Singapore, 2001.
(57) Bracewell, R. N. *Sci. Am.* **1989**, *260*, 86.
(58) Balucani, U.; Brodholt, J. P.; Vallauri, R. *J. Phys.: Condens. Matter* **1996**, *8*, 6139.
(59) Herzberg, G. *Molecular Spectra and Molecular Structure*; D. Van Nostrand: Princeton, 1968.
(60) Davis, A. R.; Chatterjee, R. M. *J. Solution Chem.* **1975**, *4*, 399.
(61) Risberg, E. D.; Eriksson, L.; Mink, J.; Pettersson, L. G. M.; Skripkin, M. Y.; Sandstrom, M. *Inorg. Chem.* **2007**, *46*, 8332.
(62) Ford, T. A. *J. Mol. Struct.* **2009**, *924*, 466.
(63) Dermota, T. E.; Hydutsky, D. P.; Bianco, N. J.; Castleman, A. W., Jr. *J. Phys. Chem. A* **2005**, *109*, 8254.
(64) Post, B.; Schwartz, R. S.; Fankuchen, I. *Acta Crystallogr.* **1952**, *5*, 372.
(65) Schomaker, V.; Stevenson, D. P. *J. Am. Chem. Soc.* **1940**, *62*, 1270.
(66) Crable, G. F.; Smith, W. V. *J. Chem. Phys.* **1951**, *19*, 502.
(67) Holder, C. H., Jr.; Fink, M. *J. Chem. Phys.* **1981**, *75*, 5323.
(68) Scott, A. P.; Radom, L. *J. Phys. Chem.* **1996**, *100*, 16502.
(69) DeFrees, D. J.; McLean, A. D. *J. Chem. Phys.* **1985**, *82*, 333.